

Fabrication of ZnO nanocatalyst as an excellent heterogeneous catalyst applicant for Methyl Orange dye degradation in aqueous medium.

Zaheer Ahmed Mahar (✉ azaheer1568@gmail.com)

Shah Abdul Latif University

Ghulam Qadir Shar

Shah Abdul Latif University

Aamna Balouch

NCEAC: University of Sindh National Centre of Excellence in Analytical Chemistry

Research Article

Keywords: ZnO/PVP nanocomposites, heterogeneous Catalysis, Chemical Degradation method, Methyl Orange

Posted Date: September 20th, 2021

DOI: <https://doi.org/10.21203/rs.3.rs-888933/v1>

License:  This work is licensed under a Creative Commons Attribution 4.0 International License.

[Read Full License](#)

Fabrication of ZnO nanocatalyst as an excellent heterogeneous catalyst applicant for Methyl Orange dye degradation in aqueous medium.

Zaheer Ahmed Mahar^{1*}, Ghulam Qadir Shar¹, Aamna Balouch²⁻³

¹Institute of Chemistry, Shah Abdul Latif University, Khairpur 66020, Sindh, Pakistan.

²National Centre of Excellence in Analytical Chemistry, University of Sindh, 76080, Jamshoro, Pakistan.

³Faculty of Science and Letters, Department of Physics Engineering, Istanbul Technical University, Maslak, 34467 Sariyer/ Istanbul Turkey

*Corresponding Email: azaheer1568@gmail.com

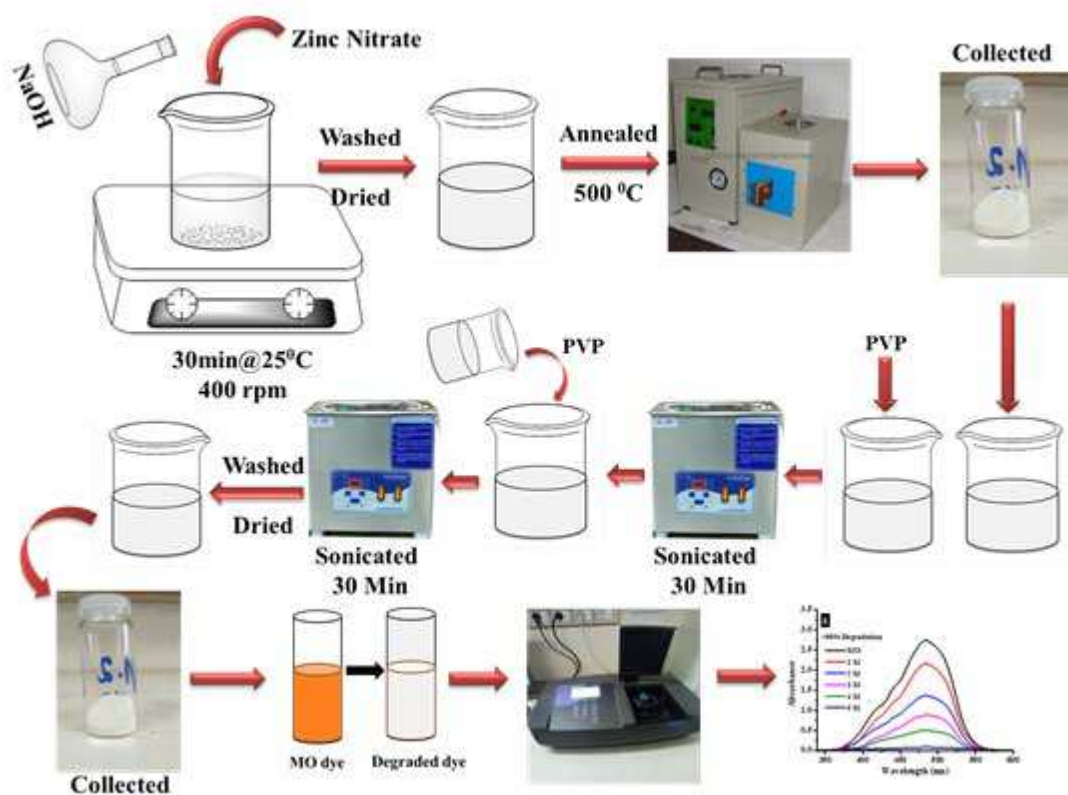
Abstract

The current paper describes the fabrication of an excellent and economical heterogeneous nanocatalyst for the degradation of methyl orange dye in aqueous medium. ZnO/PVP nanocatalyst has been successfully synthesized by the chemical degradation route, followed by ultrasonication. The size, shape and crystalline structure of synthesized ZnO/PVP nano composite was characterized by UV-visible spectroscopy, X-ray diffractometry, Dynamic Scattering Light, Zeta Potential, Fourier transform infrared spectroscopy, Scanning Electron Microscope, Energy Dispersive X-ray and X-ray photoelectron spectroscopy. To authenticate the catalytic efficiency of nanocatalyst, the fabricated ZnO/PVP nanocompoiste was screened for methyl orange dye degradation. Finally, synthesized nanocatalyst exhibited an admirable catalytic efficiency, above 98% of methyl orange degradation observed just in 90 seconds using least catalyst dose (150 μ g) in aqueous medium. The engineered ZnO/PVA nanocomposite shows several advantages over traditional methods for the degradation of hazard and toxic dyes, such as high percentage degradation, short time and minimum dose of nano catalyst and excellent reusability. It is suggested that this rare nanocatalyst may be used successfully on commercial level for degradation toxic pollutants.

Keywords: ZnO/PVP nanocomposites, heterogeneous Catalysis, Chemical Degradation method, Methyl Orange.

31

32 **Graphical Abstract**



33

34 *Scheme 1: Synthesis layout of ZnO/PVP nanocatalyst and Methyl orange degradation*
35 *mechanism.*

36

37

38

39

40

41

42

43

44

45 **Introduction**

46 The world's population is increasing globally day by day and the demand for fresh water will
47 increase in the future. As per reports of WHO, 80% of diseases are associated with water in
48 the developing countries. Polluted water causes diseases. Bacterial and viral pathogens are
49 responsible for approximately 3.3 million deaths (Ali et al., 2020). Anthropogenic activities
50 waste a lot of water with many impurities. These impurities come out from fertilizers,
51 pesticides, dyes, Heavy metal, germs, etc. These produce heavy effects and some of them
52 may be carcinogenic. These pollutants persist in colloidal, suspended or soluble form in
53 water. Dyes are being widely used by textile, leather, pharmaceuticals, and food, photography
54 and cosmetics industries. These industries have high-colored effects that can lead to water
55 pollution. Over ten thousand dyes are available commercially in the world. A dye has
56 complex structure and it creates problems in its degradation. Most of dyes are toxic and are
57 carcinogenic to both aquatic and to humans lives (Kumar et al., 2014a, Kumar et al., 2014b).
58 Dyes are responsible for lung, skin and respiratory disorders. Even a minor amount of dyes
59 can be readily noticed and could be the source for embarrassment of photosynthesis. Dyes are
60 extremely stable to the traditional methods for the entire color removal and degradation.
61 Several methods and techniques like reverse osmosis, coagulation-fluorescence, membrane
62 filtration and biological degradation, electrochemical and solvent extrusion processes are
63 used for cleaning dye waste. The increasing cost of these given methods requires alternative
64 methods that are reliable in combination with the green nature. These methods for treating
65 water are quaint. In these methods, only pollution is transferred from one stage to another.
66 This is why they face different types of pollutants that demand more treatment. The
67 chromophore setting of the dye is the traditionally homogeneous arrangement. Therefore,
68 adsorption is accepted in place to treat water containing dyes. The Adsorption technique is
69 simple, highly effective and reusable so that it is more applicable (Pinky et al., 2015, Kumar
70 et al., 2014c, Gupta et al., 2012, Ameta et al., 2013).

71 Nano materials undergo revolutionary changes in nano-technology. Nano materials are used
72 to treat water because of their attractive physico chemicals. They can be specially specific
73 and reusable legends for poisonous ions in molecules, inorganic and organic solutes in
74 aqueous media. Using new materials to purify water can create huge opportunities, as they
75 create large surface areas. Numerous properties of ZnO NPs, including electric and catalytic,
76 depend on the shape and size. Different methods can be used to produce ZnO nanoparticles
77 like thermal conduction, homogeneous precipitation, spray pyrolysis, sol-gel processing, and

78 mechanical milling, hydrothermal, microwave, reflux and chemical synthesis. ZnO is an
79 environmentally friendly material. It is used in practical applications as an effective photo
80 catalyst which is sensitive to UV light. Chemical reactions are also created by catalyst, the
81 generated electron/hole pairs. The structure of relatively harmless end products represents
82 one of the more attractive features of this method (Chen et al., 2011, Roy and Mondal, 2014).
83 Methyl orange ($C_{14}H_{14}N_3NaO_3S$) belongs to an anionic azo dye family. Methyl orange has
84 been widely used in innumerable industries including printing, paper, textile, food, leather,
85 pharmaceutical as well as photography. Conversely, methyl orange (MO) dye causes
86 environmental serious pollution, known as carcinogenic (Chen et al., 2008). MO dye is
87 soluble in water and has good stability and possesses distinct color. Photocatalytic
88 degradation of dyes containing wastes has also been extensively described (Al-Qaradawi and
89 Salman, 2002, Wang et al., 2004, Liu et al., 2006, Baiocchi et al., 2002, Kansal et al., 2007,
90 Prevot et al., 2004, Liu et al., 2005). Maximum absorption of methyl orange was reported in
91 the range of 460-470 nm. This compound is orange and red in the basic and acidic medium
92 respectively. MO belongs to group of azo dyes that are widely used for colorization in many
93 industries. ZnO/PVP nano composite were incorporated in the precipitation and ultra-
94 sonication method, and used to remove Methyl orange dye from water medium. There are a
95 large number of studied reported for the degradation of Methyl Orange by various scholars in
96 which they used cheap metal oxides as catalyst. Photo degradation of methyl orange (10
97 ppm), Congo red (10 ppm), and Eosin Y (20 ppm), dyes in existence of H_2O_2 using
98 $Fe_2Mo_3O_{12}$ catalyst with excess MoO_3 was carried out by Suresh P et al. Around 97.4%, 100,
99 and 96.6, degradation was observed within 45, 45 and 120 min, respectively (Suresh et al.,
100 2014). Additionally, Zhang & Oh (2009) investigated decomposition effect of dyes
101 underneath several circumstances. They selected non-biodegradable dyes such as Methyl
102 Blue (MB), Rhodamine B (Rh B) Methyl Orange (MO) using Fe-ACF/ TiO_2 catalyst in the
103 existence of H_2O_2 as a reducing agent (Zhang and Oh, 2009). Wang et al. synthesized ZnO
104 NPs via thermal evaporation method and chemical deposition method with numerous size
105 scales; MO degradation was investigated and results revealed 80% degradation in 120 mints
106 (Wang et al., 2007). Hong et al. reported the synthesis of Fe_3O_4/ZnO nanoparticles via
107 precipitation method and observed 83% de-colorization of methyl orange dye in 360 mints
108 (Hong et al., 2008). Fu et al. prepared ZnO-Cu NPs and 88% degradation of MO was noticed
109 in 240 mints (Fu et al., 2011). Substrate of Indium-Tin capped ZnO Nano rods was prepared
110 and investigated for the degradation of MO dye and 71% dye was degraded observed in 2.5 h
111 (Zheng et al., 2011). J Dhanalakshmi et al. reported the bromophenol blue and methyl orange

112 dyes degradation by TiO₂ catalyst, about 85.51% and 67.12% degradation was achieved in
113 240 mins using 10 mg catalyst and 10 ppm dye (Dhanalakshmi and Padiyan, 2017). Eyasu et
114 al. fabricated Cr capped ZnS NPs and reported 65% and 74.28% degradation of MO dye
115 under UV and visible radiation after at 5, respectively (Eyasu et al., 2013).

116 Catalytic degradation of Methyl Orange by ZnO/PVP nano-catalyst was carried out.
117 Conversely, the ZnO/PVP nano-catalyst has infrequently been fabricated. Upon the above
118 fact, here we proposed a simple and effective process for the photocatalytic degradation of
119 methyl orange by NaBH₄. Because of ultrafine handling, intense recycling and cost-effective
120 preparation route, low water solubility, low short-term rates and an abnormal decrease in the
121 potential for decomposition, the proposed nano-catalyst is extremely effective. Above the
122 recorded protocols, which mark the best trademarks, the nano-catalyst presented here is more
123 defined and realistic.

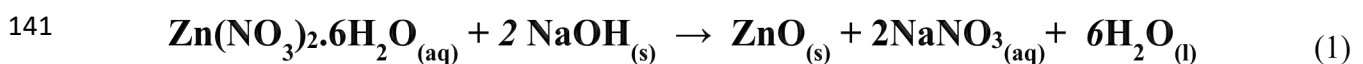
124 **Experimental work**

125 **Reagents**

126 Zinc nitrate hexahydrate salt (Zn(NO₃)₂.6H₂O), poly vinylpyrrolidone (PVP) and sodium
127 hydroxide (NaOH), Methyl orange dye (C₁₄H₁₄N₃NaO₃S) and sodium borohydrate (NaBH₄)
128 were acquired from Sigma Aldrich company and used as conventional deprived of an
129 additional sanitization. All samples using Milli Q water were prepared in aqueous medium.

130 **Fabrication of ZnO Catalyst**

131 Previously reported pattern was followed for the fabrication of Zinc Oxide NPs with slight
132 modification (Chen et al.). In experimental way, 7.1g of Zn(NO₃)₂.6H₂O was liquefied in
133 150mL twice purified water and 4g of NaOH was thawed in 50mL of Double purified water
134 independently to prepare homogenous solutions. Solution of NaOH was mixed with zinc
135 nitrate hexahydrate solution with continuous stirrer at room temperature. The impurities were
136 removed by washing particles more than one time with Double distilled and ethanol, then
137 dehydrated was performed at 70°C for 20h in furnace. Further, synthesized NPs were
138 strengthened at 550°C for 90 mints to get crystal-like particles. The obtained precipitate was
139 grinded to make particles fine. White pulverized nanoparticles was obtained and applied for
140 additional characterisation. The complete chemical reaction is given as below;



142 **Fabrication of ZnO nanostructure by PVP**

143 ZnO/PVP nano-composite was prepared by means of ultra-sonication routine. In this respect,
144 1.5g of synthesized ZnO nanoparticles was circulated in 100mL of Double distilled water and
145 0.2g of PVP were liquefied in 100mL of Double distilled and standardized in an ultra-
146 sonication bath at 30°C for 30minutes, separately. Both solutions were mixed and reserved in
147 an ultra-sonic bath for 2h to homogenies the solutions. Acquired precipitate was splashed
148 many times with double purified water and dried at 85⁰C for 24h.

149 **Methyl Orange dye degradation**

150 Commercial Methyl Orange dye (C₁₄H₁₄N₃NaO₃S, MW = 327.38g/mol) is chosen as the
151 typical pollutant to evaluate the ZnO/PVP degradation. In experimental routine, Initially, the
152 solution of MO dye and catalyst were prepared than 10 mL Methyl orange dye having 0.1
153 mM solution along with NaBH₄ (0.5 mM) was reserved in the glass vessel, and a piece of
154 ZnO/PVA was implanted in the reaction mixture sendoff for 15 seconds so as to attain
155 adsorption-desorption symmetry. 4 mL of the reaction mixture was engaged as a reference,
156 and its UV-Visible spectrum was recorded over UV-Visible spectrophotometer. Additionally,
157 different factors were optimized such as catalyst dose, reducing agent, Sun light effect, and
158 irradiation time and microwave power. Gradual degradation in the color of mixture indicated
159 methyl orange dye degraded. The percentage degradation was calculated by equation as
160 assumed under:

$$161 \quad \% \text{ Degradation} = (X_i - X_f) / X_i \times 100 \quad (2)$$

162 Here, X_i is initial and X_f is final absorbance of dyes.

163 **Characterizations techniques**

164 Firstly, UV-visible spectroscopy (Biochrom Libra S-22) were used to confirm the synthesized
165 ZnO nanostructure. Dynamic Light scattering and Zeta sizer Nano (ZS90, Malvern, UK)
166 were used to examine stability and size distribution of synthesized ZnO nanocatalyst. SEM
167 (JSM-5410LV, JEOL) technique was used to study morphology of the fabricated Zinc Oxide
168 NPS. Functional groups of prepared nanocompoiste were confirmed by FTIR spectra. In this
169 regards, Thermo Nicolet 5700, Thermo Fisher Scientific Inc. USA, FTIR Spectrophotometer
170 was used in the assortment of 4000–400cm⁻¹. Elemental ananlysis was supported out by EDX
171 technique. XPS analysis (AXIS ultra by Shimadzu equipped with dual-anode X-ray source

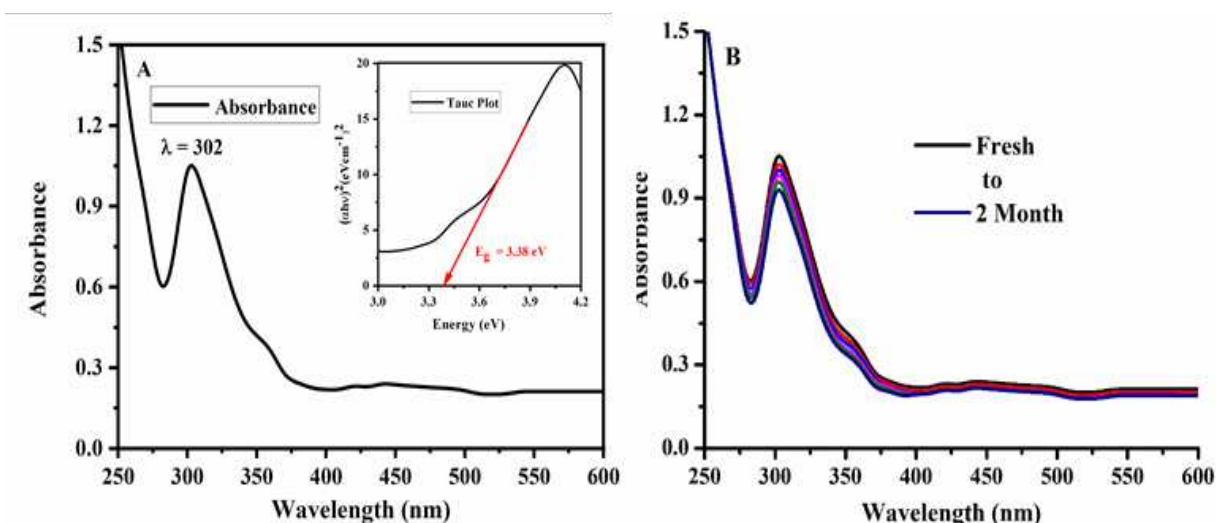
172 Al/Mg and the HAS hemispherical sector analyzer detector) was performed to investigate the
173 chemical bonding and composition of fabricated nanocatalyst. X-ray diffractometer (D/max-
174 IIB, Rigaku) was used to investigate the nanometric size, crystal-like nature and phase purity
175 with a $K\alpha_1$ Cu ($\lambda = 1.5406$ nm) at a tube voltage of 40 KV and 20 mA current.

176 Results and Discussion

177 Characterisation of synthesized catalyst

178 Nanocomposite Peak, Stability and Band Gap study

179 Catalyst was confirmed by utilizing UV-Visible technique. As shown in figure 1A, the
180 ZnO/PVP nanocomposite reveals the absorbance peak at 302 nm. While inset displayed the
181 band gap measurement of fabricated nanocomposite via Tauc's relation. About, 3.38 eV
182 direct band gap energy was calculated. Moreover, stability of prepared nanomaterial was
183 checked by interlinking the spectra of fresh and two month later recorded spectra of similar
184 nanoparticles. As shown in figure 1B, insignificant change in the peak intensity was detected
185 with the passage of time. It indicates that the fabricated catalyst is highly stable.



186

187 *Figure 1: (A) ZnONPs UV–V spectrum, inset shows Tauc plot (B) stability of nanocatalyst*

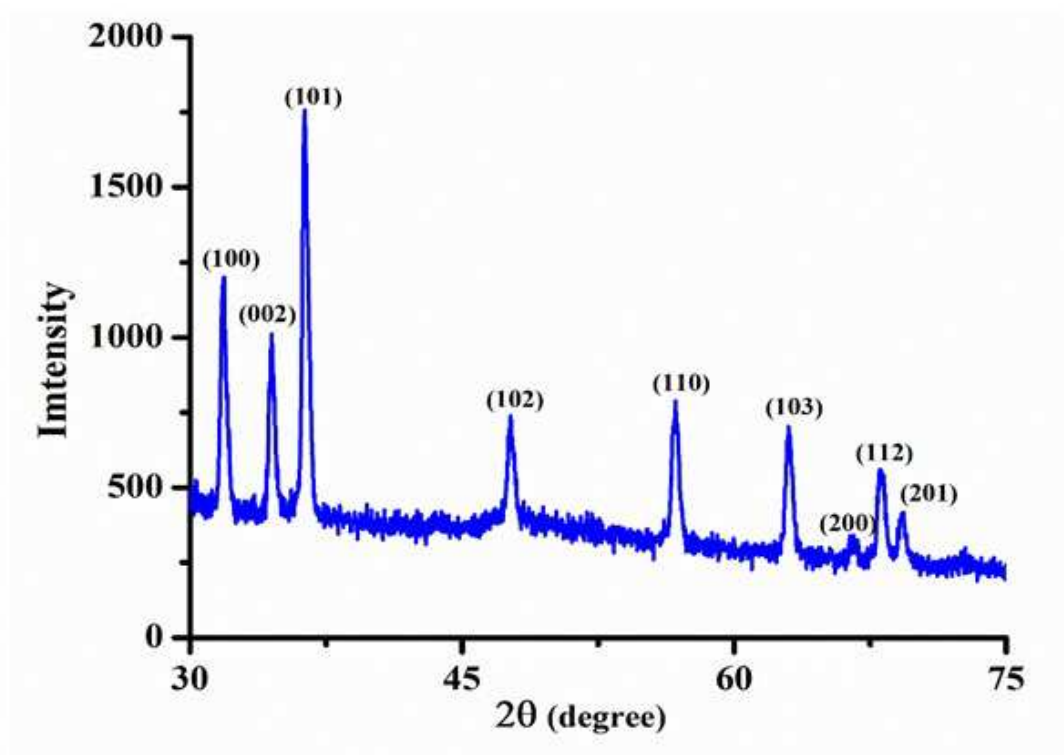
188 XRD analysis

189 The XRD array of prepared nanocatalyst is shown in Figure 2. The peaks are more exhaustive
190 and thinner suggesting a worthy crystalline nature of the prepared ZnO/ PVP nanocatlyst. The
191 corresponding pattern of nanocomposite appear at the distinctive points of crystals at $2\theta =$
192 31.79, 34.56, 36.33, 47.64, 56.74°, 63.06, 66.39, 68.05 and 69.05 in accordance with planes

193 (100), (002), (101), (102), (110), (103), (200), (112), and (201) as reported in JCPDS card
 194 (NO.36-1451) that indicates the hexagonal wurtzite assembly of Zinc Oxide NPS (Krishna
 195 Reddy et al., 2017). In XRD pattern peaks of impurities were not observed indicating that
 196 synthesized nanocomposite are highly crystalline in nature. The Debye-Scherrer principle
 197 was used to calculate the average crystalline size (L) of the nano-composite as given below
 198 (Chen et al., 2007):

$$D = \frac{k\lambda}{\beta \cos\theta}$$

200 Here D represents the crystalline size (nm), λ the wavelength (nm), K crystal shape factor, θ
 201 ($^\circ$) the Bragg diffraction angle ($^\circ$) and β FWHM (radian). The average crystalline size of
 202 fabricated nano composite was calculated about 41.2 nm.

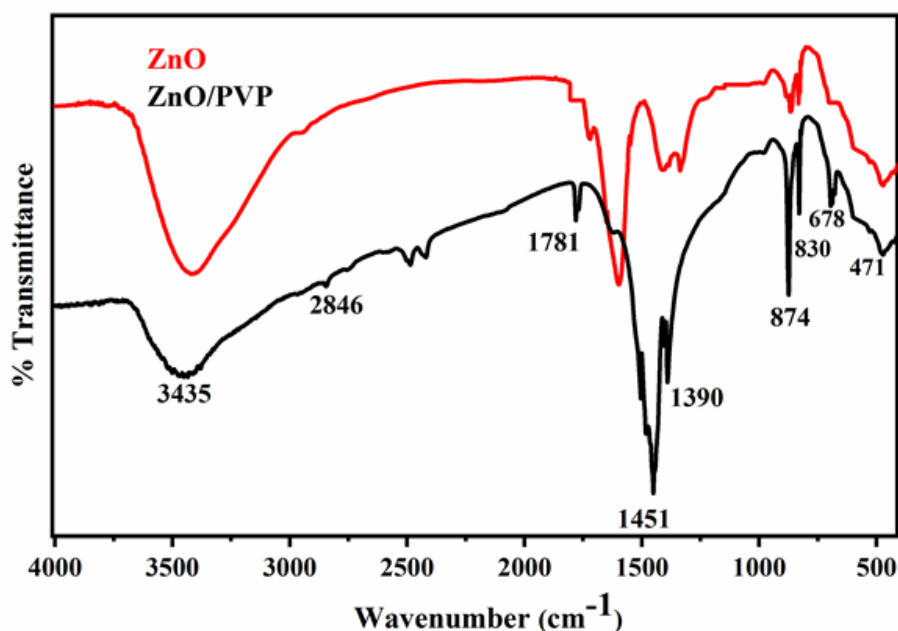


203
 204 *Figure 2: XRD pattern of catalyst*

205 **Functional group of catalyst**

206 Chemical configuration of synthesized ZnO/PVP Nano composite was investigated by FTIR
 207 as demonstrated in Figure 3. The change in our ZnO nanoparticles spectra was observed
 208 when PVP solution added that reveals the fabrication of ZnO/PVP nanostructure. The band at
 209 3435cm^{-1} and 2846cm^{-1} entrusted the stretching vibration OH ion of water adsorbed at the

210 particle's surface and of C-H bond respectively. The peaks near to 2846cm^{-1} , 1781cm^{-1} and
211 1451cm^{-1} are assigned to stretching vibration of C-H, C=O and C-N bonds correspondingly.
212 The characteristic of peak at 1390 cm^{-1} is belongs to the bond of C-H in PVP. The
213 absorption band near at 471 cm^{-1} and 678 cm^{-1} assigned to stretching vibrations of Zn-O
214 bond (Hong et al., 2009). Consequently, FTIR Spectra indicates that chemical reaction occur
215 among ZnO NPs and polymeric preservative, by synchronization of ZnO NPs with oxygen
216 and nitrogen in PVP (Ilegbusi and Trakhtenberg, 2013).



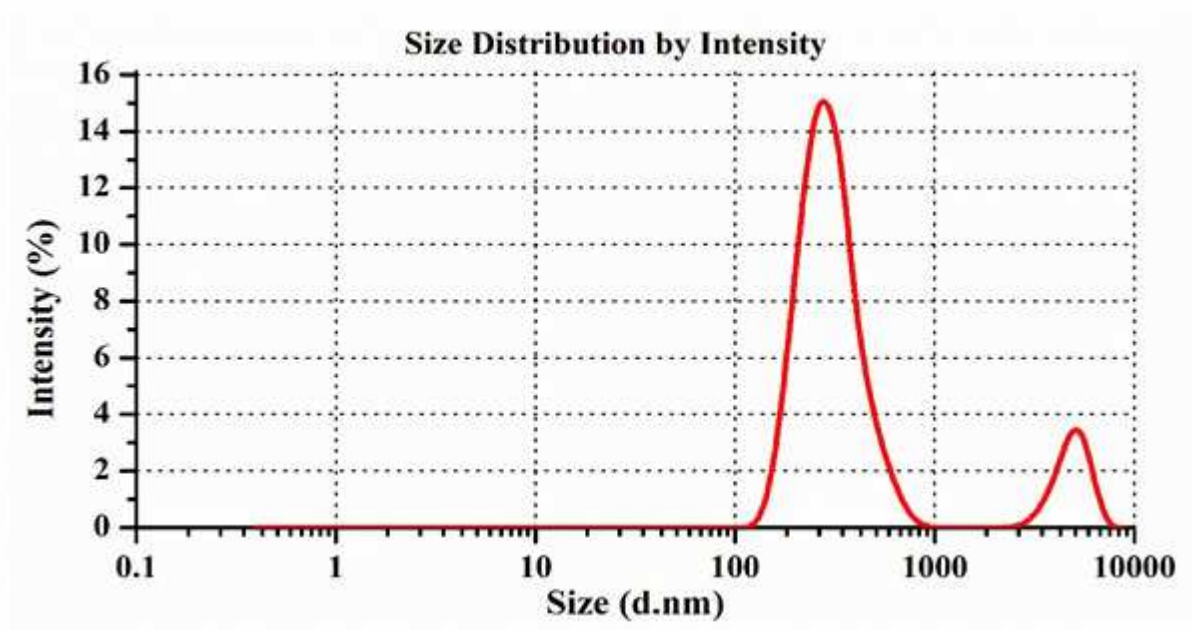
217

218 *Figure 3: FTIR spectra of catalyst*

219 **Size and charge determination of catalyst**

220 For the operative usage of metal oxide nanomaterial, the ZnO/ PVP nanocomposite must be
221 in the range of small size. The nanocomposite can be successfully obtained with properties at
222 the nanoscale and effectively applied in photocatalytic applications. The average size of
223 prepared nanocatalyst, and PDI calculated as 280 nm and 0.253 by using the DLS technology
224 (Fig: 4). On the bases of these outcomes, it is recommended that the formed nanocomposite
225 are mono dispersions and the combined size distribution of nanoparticles. In addition, ZP was
226 analyzed to uncover the surface charges obtained by Zinc oxide nanoparticles, which have
227 been used to determine the stability of the fabricated ZnO/PVP nanocatalyst. It is reported in
228 literature that the particles possess the ZP value more than + 30 mV or -30 mV have the
229 greater stability (Gautam et al., 2018). Nanoparticles have the electrostatic repulsion force
230 that depends on the surface charge of nanoparticle. The negative charge of nanoparticles

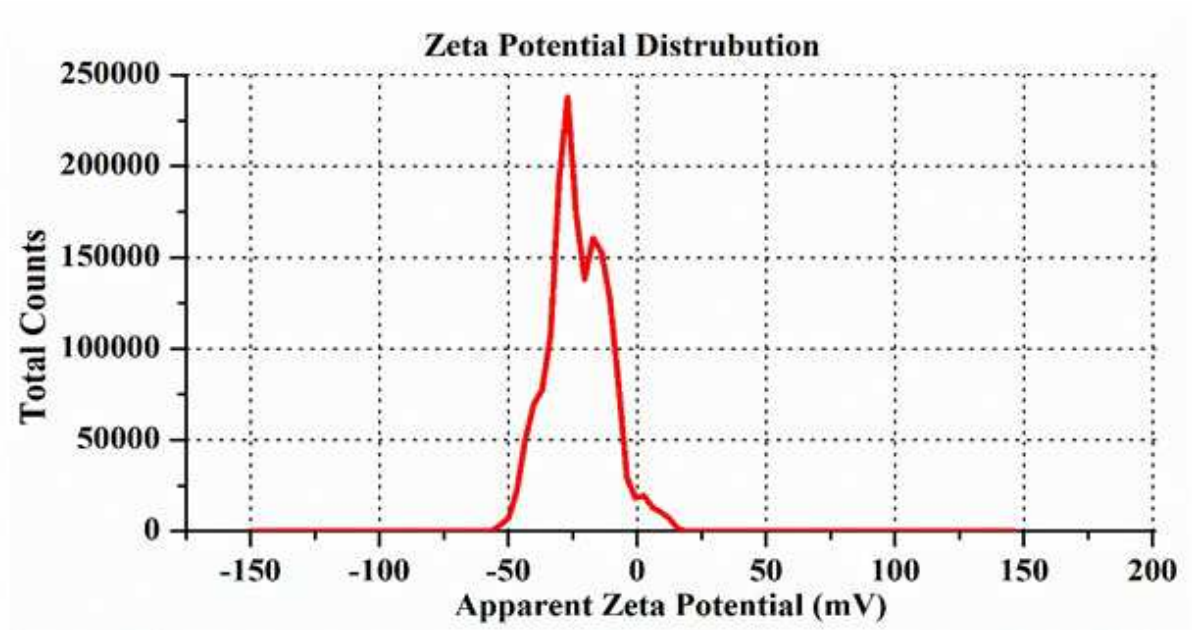
231 provide collective resistance and long-term stability. In current composition, the potential
232 value of additional negative zeta supports the movement of repulsion among nanoparticles
233 and thus improves the stability of synthetic particles. As shown in Figure 5, The Zeta
234 potential value of the prepared ZnO/PVP NCs was detected at -22.8 mV. On the behalf of
235 these outcomes it is summarized that the prepared PVP capped ZnO nanocatalyst is
236 particularly stable.



237

238

Figure 4: DSL of ZnO/PVP catalyst



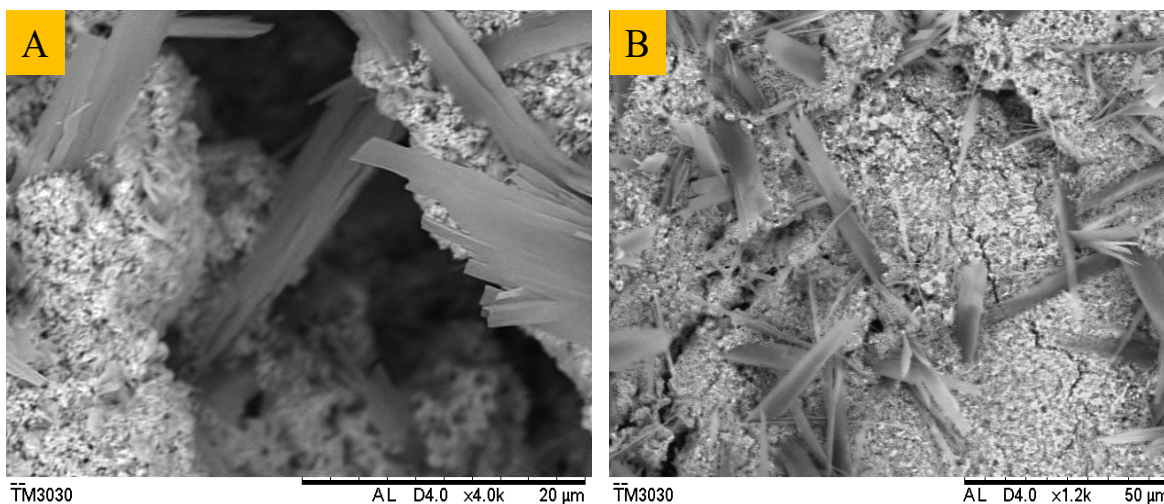
239

240

Figure 5: ZP of ZnO/PVP catalyst

241 **Surface morphology and elemental analysis of catalyst**

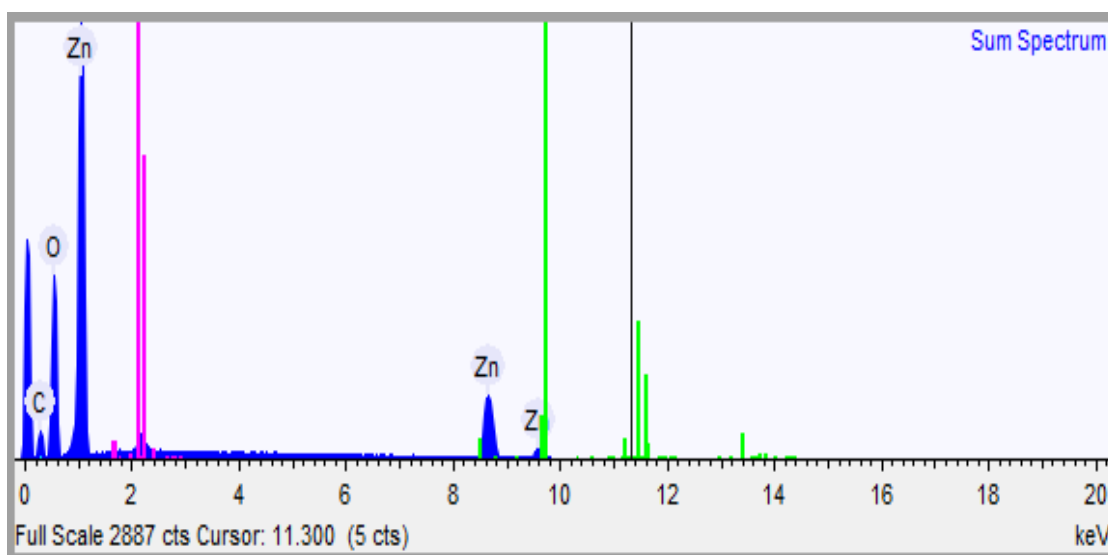
242 The morphology of the material fabricated at the nanoscale may show a significant character
243 in the catalytic reaction. In quest to investigate the geographical evaluation of a jointly
244 designed ZnO/PVP nanocomposite, SEM was performed effectively. Figure 6 (A&B) shows
245 the SEM images of synthesized ZnO/PVP nanomaterial. The synthesized nano sheets
246 smoothness proved to be a reliable and effective preparation of PVP capped ZnO on the
247 nanoscale. However, the similarity in texture shows that the synthesized particles can be used
248 for a catalytic reaction. Additionally, Elemental structure of ZnO/PVP nanocatalyst was
249 inspected via EDX study. Figure 7 exposes the presence of Zn, O and C as the main elements
250 of fabricated nanocatalyst. Resultantly, the prepared nanocomposites were found pure.



251

252

Figure 6: SEM descriptions of catalyst A. low resolution B. High resolution



253

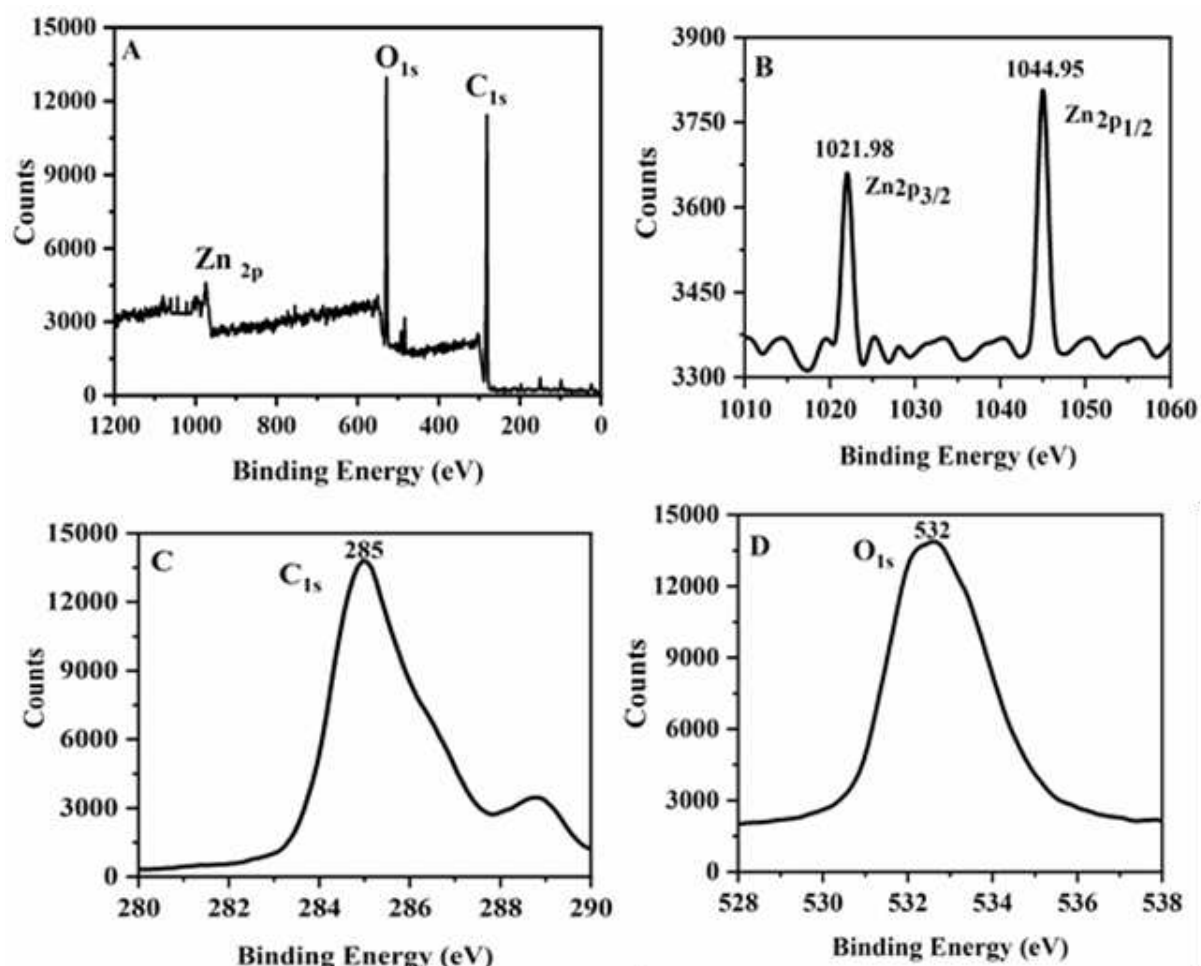
254

Figure 7: EDX pattern of catalyst

255

X-ray Photoelectron Spectroscopy Study

256 Synthesized ZnO nanocatalyst were further investigated by XPS technique (Figure 8). The
257 Binding Energy of nanocomposites at 1021.98 and 1044.95eV would assigned to Zn 2p_{3/2} and
258 Zn2p_{1/2}, respectively as displayed in Figure 8B. The Binding Energy at 285eV and 532eV are
259 linked to C1s and O1s of ZnO, respectively as exposed in Figure 8 (C&D) (Morozov et al.,
260 2015, Sa'edi et al., 2016).



261

262 *Figure 8: (A) Full XPS spectrum of ZnO/PVP nanocatalyst, (B) Zn2p (C) C1s (D) O1s*

263 **Catalytic investigation of synthesized ZnO nanocatalyst.**

264 Methyl orange (MO) dye nominated as a contaminant to assess the catalytic potency of
265 synthesized ZnO/PVP nanocomposite in presence and absence of sodium borohydare
266 (NaBH₄) as reducing agent under different circumstances. Experiment was carried out after
267 optimizing all the parameters such as reducing agent, Sun light effect, catalyst dose,
268 irradiation time and microwave power. UV-V Spectrometer was used to monitor the
269 degradation. Absorbance peak of MO dye was perceived at 464 nm (λ -max) (Radini et al.,
270 2018). During process, gradual degradation of absorption intensity with passage of reaction

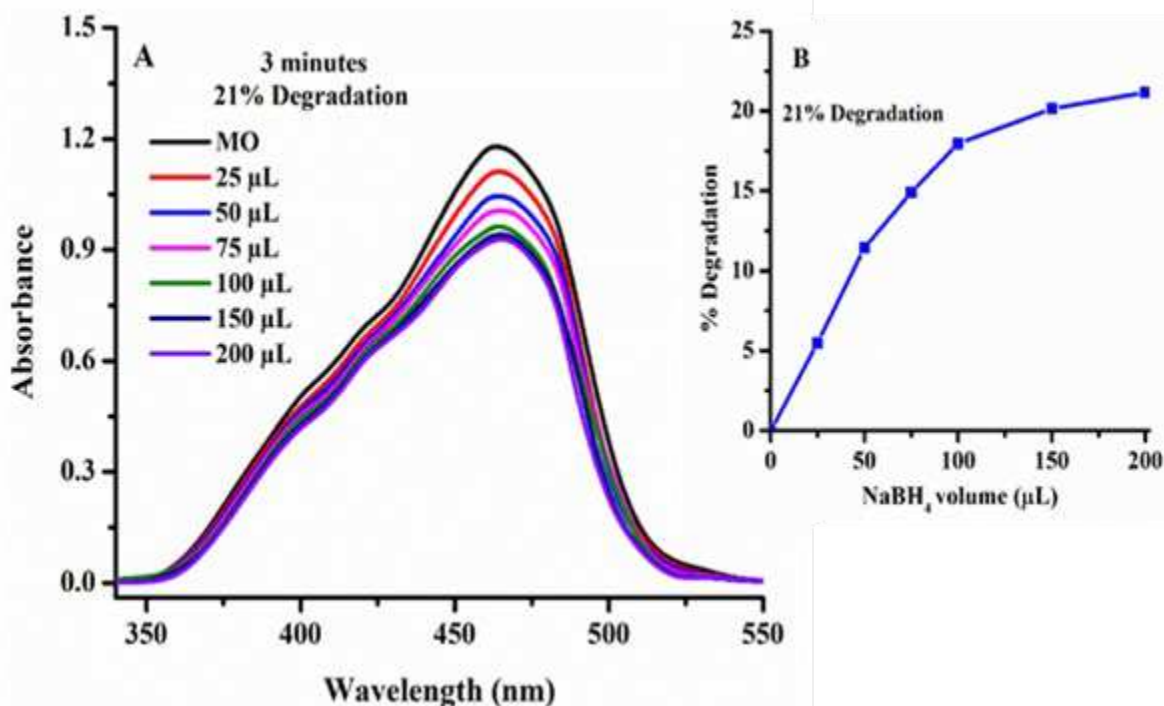
271 and color of methyl orange dye become less intensive because of MO oxidation in the
272 presence of synthesized nanocatalyst.

273

274 **Parameters Optimization study**

275 **Effect of reducing agent**

276 Sodium borohydrate is a crucial component which is very supportive to boost the degradation
277 ability of suggested nanocatalyst. The sources of the proposed proton from NaBH_4 and
278 supporting factors have been evaluated to check the performance of the proposed
279 nanocatalyst. Initially, the NaBH_4 effect was examined by adding different volumes (25–200
280 μL of 0.5 mM), at fix concentration of Methyl orange dye (0.1 mM). By increasing the
281 volume of reducing agent a significant variation was noticed in peak degradation (figure 9A).
282 Approximately, 21% the degradation in MO was detected, while no significant decrease in
283 intensity was observed upon the addition of NaBH_4 . Only 1-2% degradation was observed as
284 shown in figure 9B. Additionally, it was observed that the extensive dose of NaBH_4 didn't
285 deliver better outcomes, because of the certain boundaries that could be due to the absence of
286 any support to adsorb/capture of hydride ions. The problem was subsequently resolved by
287 adding the surface modified ZnO/PVP nanocatalyst. This assisted as a durable support for the
288 impressive deposition of hydride ions that severely degrade the MO molecule to significant
289 point.

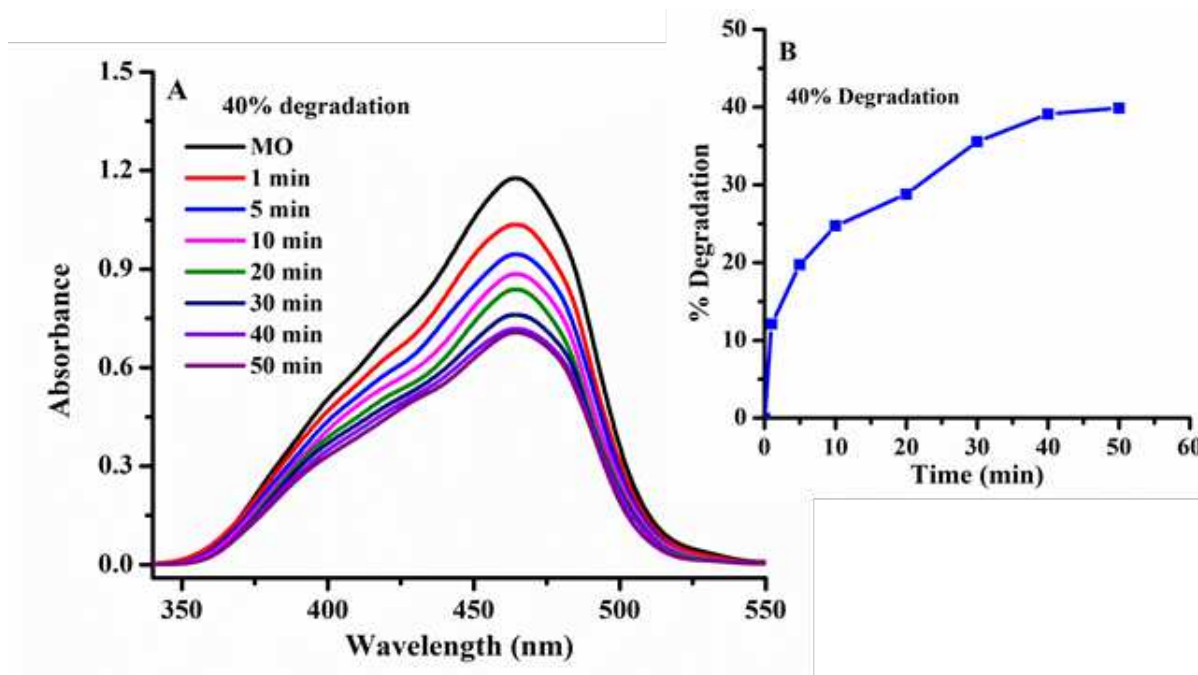


290
 291 *Figure 9: UV-Vis spectral for (A) Effect of reducing agent (0.5 mM, 25–200 μL) on the*
 292 *degradation of Methyl orange dye (0.1 mM) in without of catalyzed, utilizing 3 minutes B. %*
 293 *degradation at different volume of reducing agent*

294

295 Sunlight effect

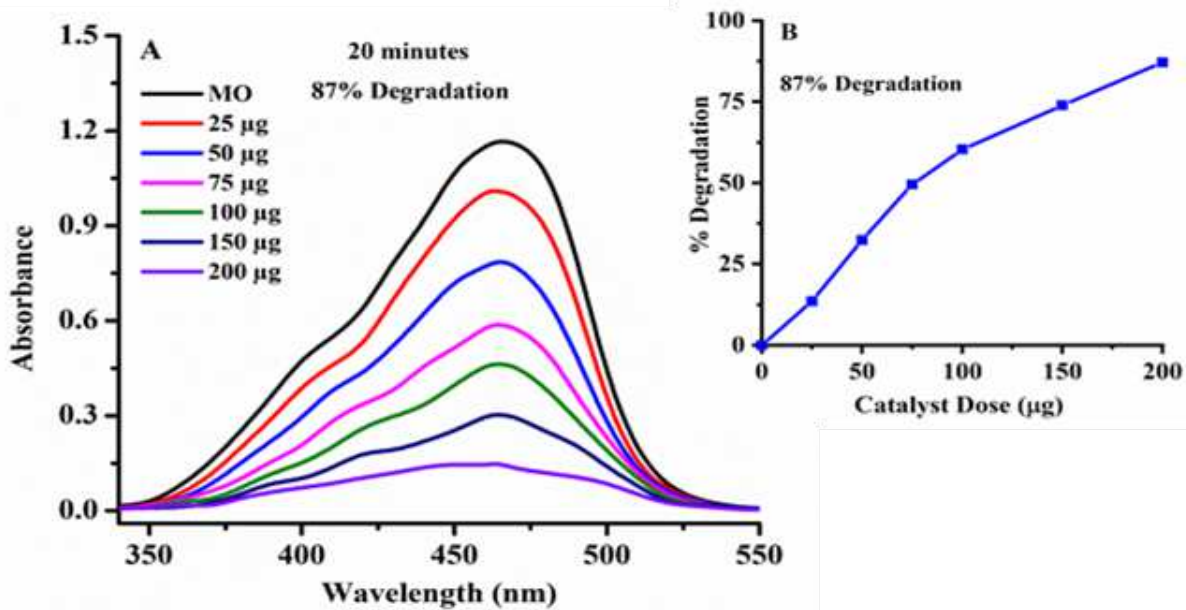
296 Secondly, the effect of sunlight was adjusted without nanocatalyst, after the reducing agent
 297 optimization (0.5 mM NaBH₄, 200 μL). In peak intensity of Methyl orange (0.1 mmol L⁻¹)
 298 notable deviation was observed. The organized solution was taken under the sun for 1 to 50
 299 minutes and noteworthy variation in peak was noticed as shown in Figure 10 (A&B). Nearly,
 300 40% methyl orange dye reduced, although no noticeable variation was detected up on
 301 succeeding additional the energy of sun on the solution; merely 3% noted. It was obviouses
 302 that putting the solution below sunlight for more period no significant variation could be
 303 spotted. Subsequently, certain additional aspects could be optimized like as nanocatalyst
 304 dosage and time with the purpose of make the work more economical.



305
 306 *Figure 10: UV-Vis spectral for A. Effect of sunlight on the degradation of Methyl orange dye*
 307 *(0.1 mM) utilizing using 0.5 mM NaBH₄, 200 μ L B. % degradation at different volume of*
 308 *reducing agent*

309 **Effect of nanocatalyst without sodium borohydride in the existence of**
 310 **sunlight**

311 After the optimization of above factors, effect of nanocatalyst was inspected in the
 312 nonexistence of NaBH₄. A noteworthy deviation was noticed in the peak intensity of methyl
 313 orange dye when arranged solution was incubated at 25–200 μ g of ZnO/PVP nanostructure
 314 and appropriate quantity of methyl orange (0.1 mM) was retained in sun irradiation for
 315 almost 20 minutes in the deficiency of NaBH₄. Approximately 85% of methyl orange dye
 316 degraded, that is fairly sufficient but time ingesting procedure (Fig.11 A&B). In order to
 317 make the work more operative and sufficient, reducing agent must be applied to acquire more
 318 degradation and to decrease the time ingesting.

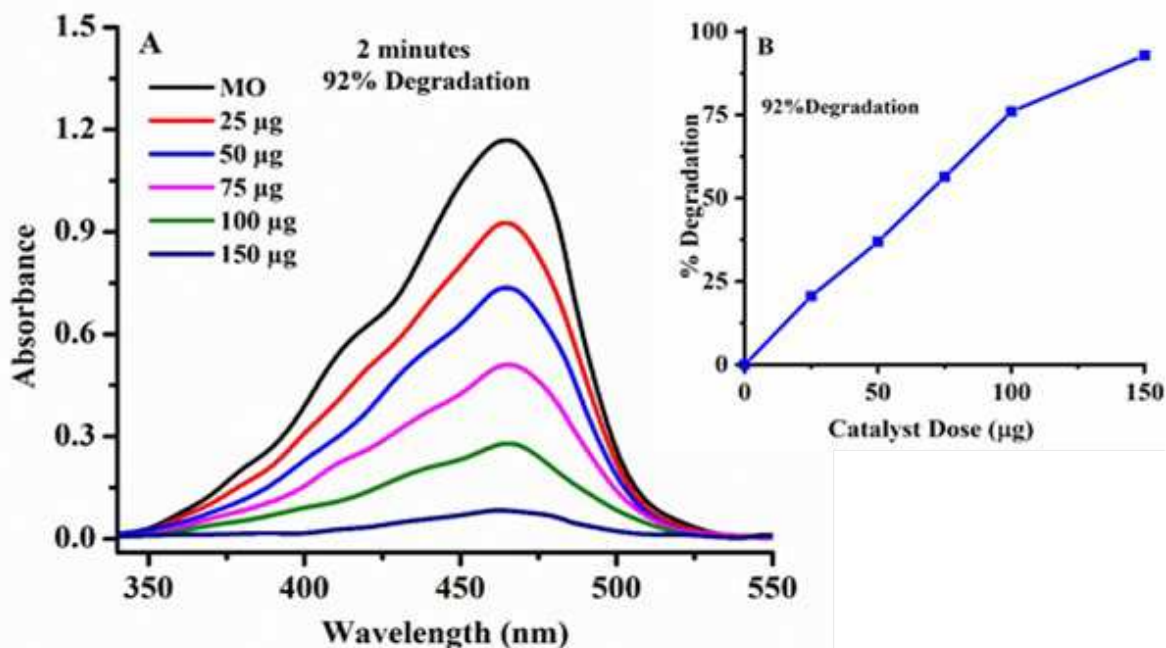


319

320 *Figure 11: A. Catalyst dose effect (25-200µg) in the absence of NaBH₄ on the degradation of*
 321 *methyl orange dye (0.1 mM) B. showing % degradation graph at different catalyst dosage in*
 322 *20 min.*

323 **Effect of Nanocatalyst with sodium borohydride in the existence of sunlight**

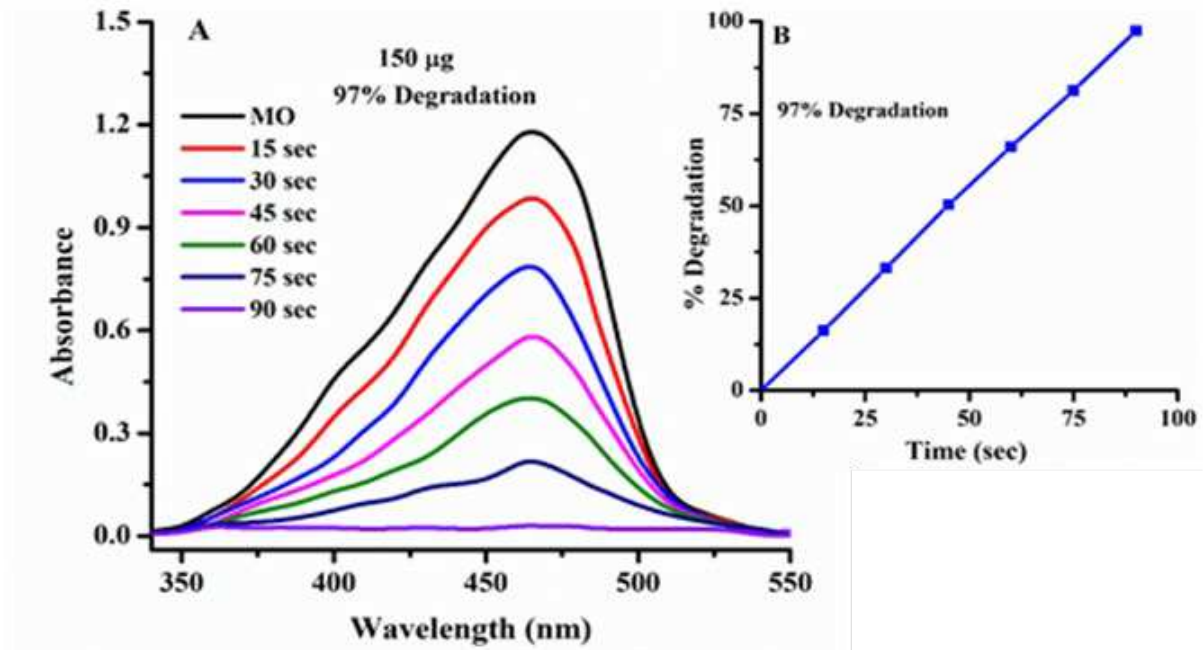
324 After elevating various factors mentioned above, the catalyst dose effect (25-150µg) was
 325 investigated in the presence of NaBH₄ (0.5 mM, 200µL) at fix concentration of methyl
 326 orange (0.1 mM). Approximately, 92% degradation was observed in peak intensity of the
 327 methyl orange dye (Figure 12 A&B). Typically Sodium borohydrate is attached to the
 328 ZnO/PVP surface, thereby increasing the activity of the nano-catalyst due to the release of
 329 proton (H⁺). Lastly, more than 90% degradation was attained by utilizing 150µg and 200µL
 330 of ZnO/PVP nanocatalyst and NaBH₄, respectively, only employing 2 minutes in every
 331 catalytic trial.



332
 333 *Figure 12: A. Catalyst dose effect (25-150µg) in the presence of NaBH₄ (0.5 mM, 200µL) on*
 334 *the degradation of methyl orange dye (0.1 mM) B. % degradation graph in 2 min.*

335 **Microwave effect study**

336 It is a critical factor that is helpful in increasing the catalytic competence of the suggested
 337 nanocomposite. Consequently, by examining all above mentioned factors, eventually the
 338 microwave power upshot desires to be inspected to make research worthy. To assess this
 339 important effect, a fixed power rate was employed (110 W) using a 150µg nano-catalyst dose
 340 and 200µL, 0.5 mM NaBH₄ volume using 0.1 mM MO dye in the nonexistence of sunlight.
 341 The effect of microwave power was monitored by increasing the sample contact duration as
 342 shown in Figure 13 (A&B). By increasing time exposure (15-90 seconds) the degradation
 343 was increased. This may be due to more energy MW power or rise in temperature. Finally,
 344 97.8% degradation was succeeded with 150µg ZnO/PVP nanocatalyst, 200µL of NaBH₄
 345 within 90 seconds microwave power.



346
 347 *Figure 13 A. Effect of MW power (110 W) on the degradation of MO dye (0.1 mM) using 0.5*
 348 *mM NaBH₄, 200µL and 150µg ZnO/PVP nanocatalyst, B. showing % degradation graph.*

349 Kinetic Study

350 In order to inspect the order of the reaction, degradation abilities and rate constant, the
 351 Lagergren kinetic model was successfully applied to examine the 1st and 2nd pseudo order
 352 reaction.

353 1st pseudo order:

$$354 \quad (q_e - qt) = \ln q_e - \frac{k_1 t}{2.303} \quad (8)$$

355 2nd pseudo order:

$$356 \quad \frac{t}{qt} = \frac{1}{k_2 q_e^2} + \frac{1}{q_e} t \quad (9)$$

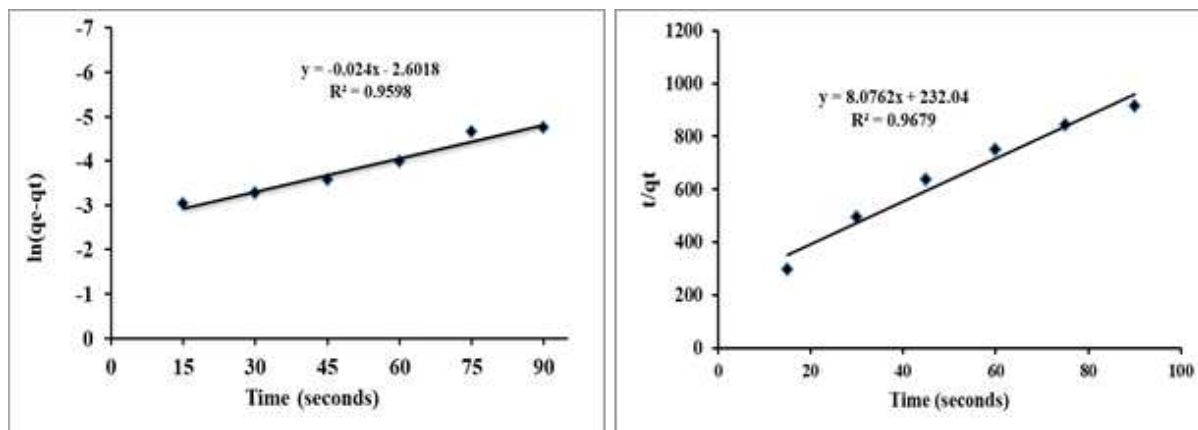
357 Where, k₁ and k₂ are rate constants for 1st and 2nd orders, respectively, and q_e, q_t and t
 358 demonstrate the equilibrium adsorbed Methyl Orange concentration (mg/g), and dye
 359 adsorbed (mg/g) over nano catalyst surface at time.

360 The graph was plotted among the equation ln (q_e-q_t) in contradiction of time (t) to
 361 investigate the adsorption potential (q_e), correlation coefficient (R) and rate constant (k) for
 362 pseudo 1st and 2nd order reaction as revealed in Figure 14 A&B. It was presumed that using
 363 the Lagergren model, the degradation reaction shadows the second order kinetics in
 364 compression of first order as exposed in Table 1.

365

Table 1: kinetic study for the degradation of Methyl Orange dye

Pseudo first order			Pseudo second order		
K_1	q_e (mg g ⁻¹)	R^2	K_2	q_e (mg g ⁻¹)	R^2
0.09851	0.04891	0.9598	0.28109	0.1238	0.9679

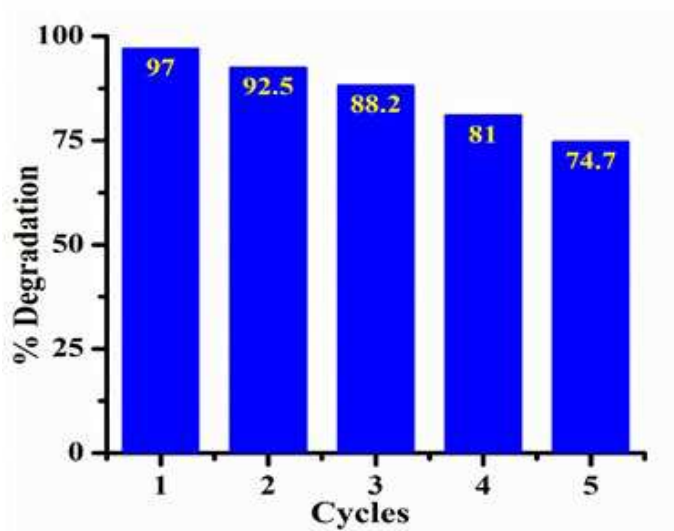


366
367

Figure 14: (A) Lagergren 1st order (B) Lagergren 2nd order for ZnO/PVP nano particles

368 **Reusability investigation**

369 The reusability and restoration of the CuO/PVA nanocatalyst is examined for the degradation
 370 of dye by execution of recycling investigates using NaBH₄. As exposed in Figure 15, there is
 371 no substantial variation in the catalytic activity of nanocatalyst after five successive phases. It
 372 demonstrates the great stability of the synthesized catalyst.



373

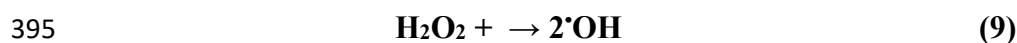
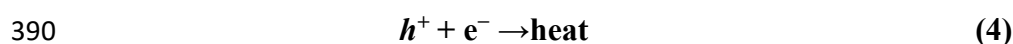
374

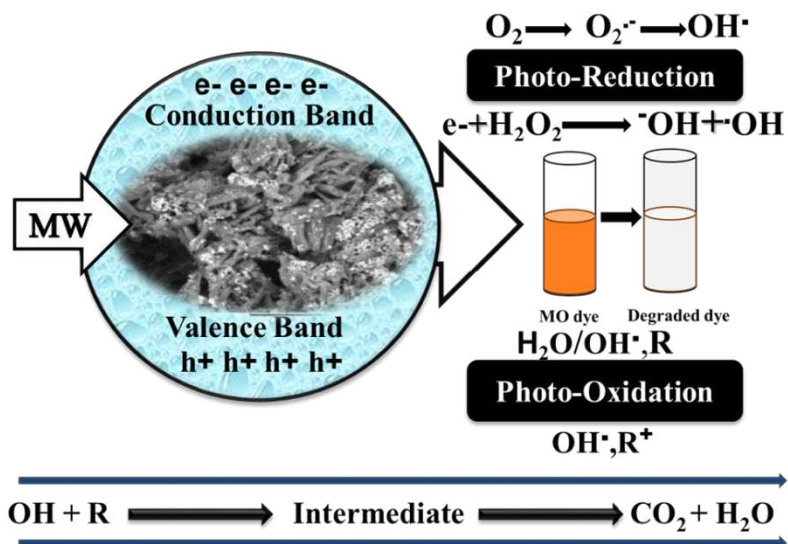
Figure 15: Reusability cycle of catalyst

375

376 **Methyl Orange dye degradation mechanism**

377 The degradation mechanism of dyes in the presence of catalysts was proposed by the earlier
378 reported (Veerakumar et al., 2015). The degradation mechanism of methyl orange with
379 ZnO/PVP nanocatalyst is revealed in Figure 16. The process comprises the transfer of
380 electron through the surface of catalyst from the valence to conduction band with
381 Microwave/Sunlight. These electrons separately can interact or recombine with other
382 molecules. On the surface of catalyst, the H₂O molecules and holes created can interact and
383 produces the hydroxide ions although superoxide anion formed when electrons are captured
384 by adsorbed oxygen. The resultant ions may generates more peroxide in the presence of
385 strong oxidizing scavenger. Being a strong oxidizing agent hydroxyl radical attack on the
386 molecules of dye and forms oxidized product as exposed in figure 16. The summary of
387 reaction is described below and possible fragmentation of methyl orange dye is similarly
388 assumed in Fig. 17

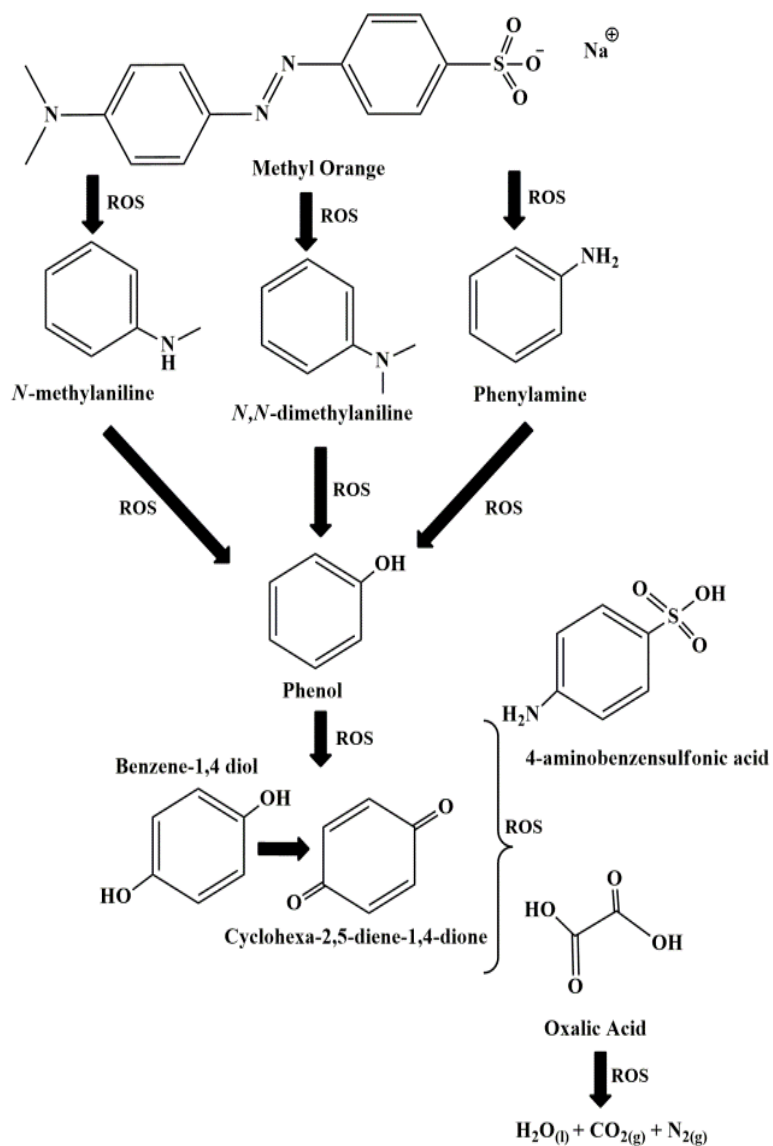




397

398

Figure 16: Schematic diagram for the degradation mechanism of MO dye



399

400

Figure 17: Fragments of methyl orange dye

401 **Evaluation of ZnO/ PVP nanocatalyst with testified work**

402 Eventually, amongst numerous nanocomposite ZnO/PVP nanocatalyst has excellent catalytic
403 activity for degradation/degradation of MO dye than the earlier conveyed work as table 2
404 shows. Examination of the reported anomalous literature proves that our recommended
405 nanocatalyst is very effective and discriminating postulant in relations of maximal %
406 degradation of methyl orange below infinitesimal catalyst dose and reducing agent dose in
407 just 90 seconds. Various types of nanocatalyst were synthesized and their catalytic
408 degradation was investigated under different conditions. However, the reported work couldn't
409 reach the 85% degradation. On the other side, we have oppressed the simplest ZnO/ PVP
410 nanocomposite and more than 97.8% degradation was observed in just 90 seconds. Based on
411 the above facts we have proposed the prepared ZnO/PVP nanocomposite and it could be a
412 major aspirant for the de-colorization of MO dye and other pollutants.

413 **Table 2:** Evaluation of ZnO/ PVP nanocatalyst with testified work

Catalyst	Catalyst Dose	Dye Conc:	% Degradation	Time	Reference
Fe ₃ O ₄ /ZnO	0.075 g	20 ppm	83	360 min	(Hong et al., 2008)
TiO ₂ NPs	10 mg	10 ppm	67.12	240 min	(Dhanalakshmi and Padiyan, 2017)
ZnO NPs	0.3 g/L	20 mg/L	80	120 min	(Wang et al., 2007)
Cr-ZnS NPs	0.5g/100ml	2.5 × 10 ⁻⁴ M	74.28	300 min	(Eyasu et al., 2013)
ZnO/PVP	150 µg	0.1 mM	97.8	90 sec	Present study

414 **Conclusion**

415 In summary, simple, low-cost and reliable method is adopted to synthesize the ZnO/PVP
416 nanocatalysts with an excellent catalytic performance in current study, and catalyst was
417 characterized via different techniques. The synthesized catalyst was screened for the
418 degradation of MO dye an aqueous medium in the existence of sodium borohydate at
419 optimized conditions. In the prearranged circumstances, more than 97.8% of degradation was
420 attained just in 90 seconds of reaction. According to our best knowledge its first analysis of
421 methyl orange dye photocatalytic degradation by ZnO/PVP nanocomposite as nanocatalyst.

422 The proposed method is best in terms of simple, operative cost and favored economically,
423 reproducible and excellent in reusability. On the bases of above facts, the synthesized PVP
424 capped ZnO nano-composite is suggested for degradation of toxic contaminates at
425 commercial level.

426 **Declarations**

427 **Ethics approval and consent to participate**

428 Not applicable.

429 **Consent for publication**

430 Not applicable.

431 **Competing interests**

432 The authors declare that they have no competing interests

433 **Data Availability**

434 All data that support the findings of this work are contained within the article.

435 **Funding**

436 Not applicable.

437 **Author information**

438 **Affiliations**

439 ¹Institute of Chemistry, Shah Abdul Latif University, Khairpur 66020, Sindh, Pakistan.

440 ²National Centre of Excellence in Analytical Chemistry, University of Sindh, 76080,
441 Jamshoro, Pakistan.

442 ³Faculty of Science and Letters, Department of Physics Engineering, Istanbul Technical
443 University, Maslak, 34467 Sariyer/ Istanbul Turkey

444 **Contributions**

445 Zaheer Ahmed Mahar: Performed Experimental work and also took part in writing portion,
446 Ghulam Qadir Shar: Supervisor help in manuscript designing and revision and Aamna
447 Blouch: Co-Supervisor gave a placement at laboratory and facilitate with chemicals and
448 glassware. And also help in manuscript and experimental designing. All authors read and
449 approved the final manuscript.

450 **References**

- 451 AL-QARADAWI, S. & SALMAN, S. R. 2002. Photocatalytic degradation of methyl orange
452 as a model compound. *Journal of Photochemistry and Photobiology A: Chemistry*,
453 148, 161-168.
- 454 ALI, M. A. M., ALSABAGH, A. M., SABAA, M. W., EL-SALAMONY, R. A.,
455 MOHAMED, R. R. & MORSI, R. E. 2020. Polyacrylamide hybrid nanocomposites
456 hydrogels for efficient water treatment. *Iranian Polymer Journal*, 29, 455-466.
- 457 AMETA, A., AMETA, R. & AHUJA, M. 2013. Photocatalytic degradation of methylene blue
458 over ferric tungstate. *Scientific Reviews & Chemical Communications*, 3, 172-180.
- 459 BAIOCCHI, C., BRUSSINO, M. C., PRAMAURO, E., PREVOT, A. B., PALMISANO, L.
460 & MARCÌ, G. 2002. Characterization of methyl orange and its photocatalytic
461 degradation products by HPLC/UV–VIS diode array and atmospheric pressure
462 ionization quadrupole ion trap mass spectrometry. *International Journal of Mass
463 Spectrometry*, 214, 247-256.
- 464 CHEN, C., LIU, J., LIU, P. & YU, B. 2011. Investigation of photocatalytic degradation of
465 methyl orange by using nano-sized ZnO catalysts. *Advances in Chemical Engineering
466 and Science*, 1, 9.
- 467 CHEN, C., LIU, P., LIU, J. & YU, B. The Investigation of Photocatalytic Activity of Nano-
468 Sized ZnO Particles Synthesized by a Direct Precipitation Method for Degradation of
469 Methyl Orange. *submitted to Journal of Photochemistry and Photobiology A:
470 Chemistry*.

- 471 CHEN, C., YU, B., LIU, J., DAI, Q. & ZHU, Y. 2007. Investigation of ZnO films on Si<
472 111> substrate grown by low energy O⁺ assisted pulse laser deposited technology.
473 *Materials Letters*, 61, 2961-2964.
- 474 CHEN, T., ZHENG, Y., LIN, J.-M. & CHEN, G. 2008. Study on the photocatalytic
475 degradation of methyl orange in water using Ag/ZnO as catalyst by liquid
476 chromatography electrospray ionization ion-trap mass spectrometry. *Journal of the*
477 *American Society for Mass Spectrometry*, 19, 997-1003.
- 478 DHANALAKSHMI, J. & PADIYAN, D. P. 2017. Photocatalytic degradation of methyl
479 orange and bromophenol blue dyes in water using sol-gel synthesized TiO₂
480 nanoparticles. *Materials Research Express*, 4, 095020.
- 481 EYASU, A., YADAV, O. & BACHHETI, R. 2013. Photocatalytic degradation of methyl
482 orange dye using Cr-doped ZnS nanoparticles under visible radiation. *Int. J. Chem.*
483 *Tech. Res*, 5, 1452-1461.
- 484 FU, M., LI, Y., LU, P., LIU, J. & DONG, F. 2011. Sol-gel preparation and enhanced
485 photocatalytic performance of Cu-doped ZnO nanoparticles. *Applied Surface Science*,
486 258, 1587-1591.
- 487 GAUTAM, A., RAY, A., MUKHERJEE, S., DAS, S., PAL, K., DAS, S., KARMAKAR, P.,
488 RAY, M. & RAY, S. 2018. Immunotoxicity of copper nanoparticle and copper sulfate
489 in a common Indian earthworm. *Ecotoxicology and environmental safety*, 148, 620-
490 631.
- 491 GUPTA, V. K., JAIN, R., MITTAL, A., SALEH, T. A., NAYAK, A., AGARWAL, S. &
492 SIKARWAR, S. 2012. Photo-catalytic degradation of toxic dye amaranth on
493 TiO₂/UV in aqueous suspensions. *Materials Science and Engineering: C*, 32, 12-17.
- 494 HONG, R., LI, J., CHEN, L., LIU, D., LI, H., ZHENG, Y. & DING, J. 2009. Synthesis,
495 surface modification and photocatalytic property of ZnO nanoparticles. *Powder*
496 *Technology*, 189, 426-432.
- 497 HONG, R., ZHANG, S., DI, G., LI, H., ZHENG, Y., DING, J. & WEI, D. 2008. Preparation,
498 characterization and application of Fe₃O₄/ZnO core/shell magnetic nanoparticles.
499 *Materials research bulletin*, 43, 2457-2468.

- 500 ILEGBUSI, O. J. & TRAKHTENBERG, L. 2013. Synthesis and conductometric property of
501 sol-gel-derived ZnO/PVP nano hybrid films. *Journal of materials engineering and*
502 *performance*, 22, 911-915.
- 503 KANSAL, S., SINGH, M. & SUD, D. 2007. Studies on photodegradation of two commercial
504 dyes in aqueous phase using different photocatalysts. *Journal of hazardous materials*,
505 141, 581-590.
- 506 KRISHNA REDDY, G., JAGANNATHA REDDY, A., HARI KRISHNA, R.,
507 NAGABHUSHANA, B. & GOPAL, G. R. 2017. Luminescence and spectroscopic
508 investigations on Gd³⁺ doped ZnO nanophosphor. *Journal of Asian Ceramic*
509 *Societies*, 5, 350-356.
- 510 KUMAR, S., BHANJANA, G., DILBAGHI, N. & UMAR, A. 2014a. Multi walled carbon
511 nanotubes as sorbent for removal of crystal violet. *Journal of Nanoscience and*
512 *Nanotechnology*, 14, 7054-7059.
- 513 KUMAR, S., BHANJANA, G., JANGRA, K., DILBAGHI, N. & UMAR, A. 2014b.
514 Utilization of carbon nanotubes for the removal of rhodamine B dye from aqueous
515 solutions. *Journal of Nanoscience and Nanotechnology*, 14, 4331-4336.
- 516 KUMAR, S., BHANJANA, G., KUMAR, R. & DILBAGHI, N. 2014c. Removal of anionic
517 dye amido black by multi-walled carbon nanotubes. *Journal of Nanoengineering and*
518 *Nanomanufacturing*, 4, 158-163.
- 519 LIU, S., YANG, J.-H. & CHOY, J.-H. 2006. Microporous SiO₂-TiO₂ nanosols pillared
520 montmorillonite for photocatalytic decomposition of methyl orange. *Journal of*
521 *Photochemistry and Photobiology A: Chemistry*, 179, 75-80.
- 522 LIU, Y., CHEN, X., LI, J. & BURDA, C. 2005. Photocatalytic degradation of azo dyes by
523 nitrogen-doped TiO₂ nanocatalysts. *Chemosphere*, 61, 11-18.
- 524 MOROZOV, I. G., BELOUSOVA, O., ORTEGA, D., MAFINA, M.-K. & KUZNETCOV,
525 M. 2015. Structural, optical, XPS and magnetic properties of Zn particles capped by
526 ZnO nanoparticles. *Journal of Alloys and Compounds*, 633, 237-245.

- 527 PINKY, S., FERDUSH, A., KURNY, A. & GULSHAN, F. 2015. Photo Degradation of
528 Industrial Dye Using ZnO as Photo Catalyst. *International Journal of Innovative*
529 *Research in Science, Engineering and Technology*, 4, 9986-9992.
- 530 PREVOT, A. B., BASSO, A., BAIOCCHI, C., PAZZI, M., MARCÍ, G., AUGUGLIARO, V.,
531 PALMISANO, L. & PRAMAURO, E. 2004. Analytical control of photocatalytic
532 treatments: degradation of a sulfonated azo dye. *Analytical and bioanalytical*
533 *chemistry*, 378, 214-220.
- 534 RADINI, I. A., HASAN, N., MALIK, M. A. & KHAN, Z. 2018. Biosynthesis of iron
535 nanoparticles using *Trigonella foenum-graecum* seed extract for photocatalytic methyl
536 orange dye degradation and antibacterial applications. *Journal of Photochemistry and*
537 *Photobiology B: Biology*, 183, 154-163.
- 538 ROY, T. K. & MONDAL, N. K. 2014. Photocatalytic degradation of congo red dye on
539 thermally activated zinc oxide. *International Journal of Scientific Research in*
540 *Environmental Sciences*, 2, 457.
- 541 SAÁEDI, A., YOUSEFI, R., JAMALI-SHEINI, F., ZAK, A. K., CHERAGHIZADE, M.,
542 MAHMOUDIAN, M., BAGHCHESARA, M. A. & DEZAKI, A. S. 2016. XPS
543 studies and photocurrent applications of alkali-metals-doped ZnO nanoparticles under
544 visible illumination conditions. *Physica E: Low-dimensional Systems and*
545 *Nanostructures*, 79, 113-118.
- 546 SURESH, P., KUMARI, U. S., RAO, T. S. & RAO, A. P. 2014. Rapid visible light photo
547 catalytic degradation of Eosin Y, Congo red and Methyl orange with Fe₂Mo₃O₁₂ and
548 MoO₃. *J. Aplicble. Chem*, 3, 2047-2054.
- 549 VEERAKUMAR, P., CHEN, S.-M., MADHU, R., VEERAMANI, V., HUNG, C.-T. & LIU,
550 S.-B. 2015. Nickel nanoparticle-decorated porous carbons for highly active catalytic
551 reduction of organic dyes and sensitive detection of Hg (II) ions. *ACS Applied*
552 *Materials & Interfaces*, 7, 24810-24821.
- 553 WANG, C., WANG, X., XU, B.-Q., ZHAO, J., MAI, B., SHENG, G. & FU, J. 2004.
554 Enhanced photocatalytic performance of nanosized coupled ZnO/SnO₂ photocatalysts
555 for methyl orange degradation. *Journal of Photochemistry and Photobiology A:*
556 *Chemistry*, 168, 47-52.

- 557 WANG, H., XIE, C., ZHANG, W., CAI, S., YANG, Z. & GUI, Y. 2007. Comparison of dye
558 degradation efficiency using ZnO powders with various size scales. *Journal of*
559 *hazardous materials*, 141, 645-652.
- 560 ZHANG, K. & OH, W.-C. 2009. The photocatalytic decomposition of different organic dyes
561 under UV irradiation with and without H₂O₂ on Fe-ACF/TiO₂ photocatalysts.
562 *Journal of the Korean Ceramic Society*, 46, 561-567.
- 563 ZHENG, J., JIANG, Q. & LIAN, J. 2011. Synthesis and optical properties of ZnO nanorods
564 on indium tin oxide substrate. *Applied Surface Science*, 258, 93-97.
- 565